Combined intracellular three-dimensional imaging and selective nanosurgery by a nonlinear microscope

Leonardo Sacconi
University of Trento
via Sommarive 14
38050 Povo (TN), Italy

Iva M. Tolić-Nørrelykke
European Laboratory for Non-linear Spectroscopy
via Nello Carrara 1
50019 Sesto Fiorentino (FI), Italy
and
Rugjer Bošković Institute
Bijenička 54
10000 Zagreb, Croatia

Renzo Antolini
University of Trento
via Sommarive 14
38050 Trento, Italy

Francesco S. Pavone
European Laboratory for Non-linear Spectroscopy
via Nello Carrara 1
50019 Florence, Italy
and
University of Florence and INFM Sezione di Firenze
Department of Physics
via Sansone 1
50019 Florence, Italy
E-mail: pavone@lens.unifi.it

Abstract. We use near-IR femtosecond laser pulses for a combination of microscopy and nanosurgery on fluorescently labeled structures within living cells. Three-dimensional reconstructions of microtubule structures tagged with green fluorescent protein (GFP) are made during different phases of the cell cycle. Further, the microtubules are dissected using the same laser beam but with a higher laser power than for microscopy. We establish the viability of this technique for the cells of a fission yeast, which is a common model to study the mechanics of cell division. We show that nanosurgery can be performed with submicrometer precision and without visible collateral damage to the cell. The energy is primarily absorbed by the GFP molecules, and not by other native structures in the cell. GFP is particularly suitable for multiphoton excitation, as its excitation wavelength near 900 nm is benign for most cellular structures. The ability to use GFP to label structures for destruction by multiphoton excitation may be a valuable tool in cell biology. [DOI: 10.1117/1.1854675]

Keywords: two-photon excitation; laser nanosurgery; green fluorescent protein; microtubules.

Paper 04027 received Mar. 1, 2004; revised manuscript received May 27, 2004; accepted for publication May 28, 2004; published online Feb. 3, 2005.

1 Introduction

Nonlinear microscopy achieves a high axial resolution and consequently the 3-D imaging capability of confocal microscopy without the use of a confocal aperture.[1] The 3-D fluorescence imaging based on nonlinear fluorophore excitation enables a number of applications in life science.[2] For example, multiphoton and second-harmonic generation microscopy is well suited for high-resolution imaging of intrinsic molecular signals in living cells and tissues.[3] Further, multiphoton imaging has been used to study cell motility[4] and the distribution of a neurotransmitter in living cells.[5]

Laser nanosurgery is an important tool in cell biology for dissection or knock-out of specific structures without using genetic methods or chemical agents.[6] UV lasers have been used to dissect mitotic spindles.[7,8] The selectivity of the nanosurgery has been enhanced by tagging specific cellular components with green fluorescence protein (GFP), which were then destroyed with nanosecond pulses of high-intensity green laser light.[9] Recently, near-IR (NIR) femtosecond laser pulses have been used to dissect isolated human chromosomes[10] as well as plant cell walls and single plastids.[11] The cut size was below 200 nm in those experiments.

Here, we report on the use of a combined NIR 3-D microscopy and selective nanosurgery of GFP-labeled structures within living cells. The object of the imaging and nanosurgery were microtubules in fission yeast cells. Lately we used this method to investigate the force balance on the yeast mitotic spindle (a structure composed of microtubules) and the mechanism of the spindle positioning and elongation.[12] This paper is structured as follows. First, we show a 3-D reconstruction of microtubule structures during different phases of the cell cycle in fission yeast.[13] Next, we show combined imaging and intracellular nanosurgery on the microtubules. Finally, we analyze the physics of the nanosurgery phenomena.

2 Materials and Methods

2.1 *Cell Preparation*

The *Schizosaccharomyces pombe* strain SP837 (*h*^{90} *leu1-32 ura4-D18 ade6-216*) was transformed[14] with the GFP-*α*2-tubulin fusion construct pDQ105. The cells were cultured at 30°C on a synthetic drop-out medium lacking leucine (AA-

Address all correspondence to Francesco S. Pavone, European Laboratory for Non-linear Spectroscopy, via Nello Carrara 1, 50019 Sesto Fiorentino (FI), Italy. Tel: +39-55-457-2480; Fax: +39-55-457-2451; E-mail: pavone@lens.unifi.it

1083-3668/2005/$22.00 © 2005 SPIE

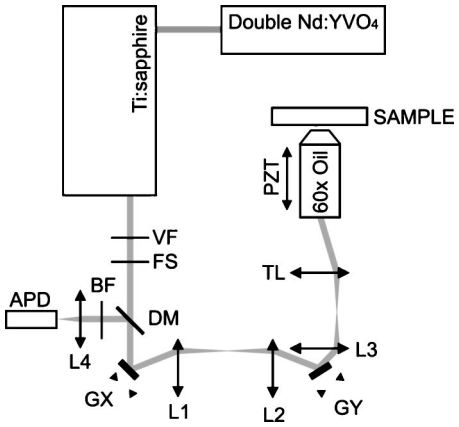

Fig. 1 Experimental setup for combined two-photon microscopy and laser nanosurgery.

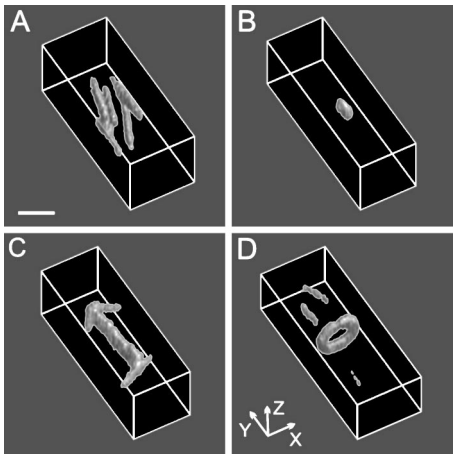

Fig. 2 A 3-D reconstruction of microtubules in different phases of the yeast cell cycle. Fission yeast cells are cylindrically shaped, with a size that fits inside the bounding box (black). (a) Five microtubules in an interphase cell, where the microtubules are roughly parallel to the long cell axis; (b) microtubules in prophase, the long interphase microtubules are absent, whereas a short mitotic spindle has formed inside the nucleus; (c) Anaphase B spindle with two astral microtubules extending from each of the two spindle poles; and (d) Postanaphase array of microtubules and the equatorial microtubule ring. Pixel dimensions was 50 nm in the *x-y* plane and 500 nm in the *z* direction, the excitation wavelength was 880 nm, the laser power was 1 mW in the sample, and the integration time for each pixel was 2.5 μs; scale bar is 2 μm.

leu) plus 2 μM of thiamine. Before microscopy, the cells were resuspended in liquid AA medium and mounted on a coverslip covered with poly-L-lysine (10 mg/ml, Sigma). Experiments were performed at room temperature. To visualize the nuclear envelope, the preceding strain was transformed[15] with the GFP-fusion construct TA22 and cultured at 30°C on AA-leu medium.

2.2 *Experimental Setup*

A scheme of the two-photon microscope is shown in Fig. 1. The expanded beam of a mode-locked titanium-sapphire laser (Mira 900F, Coherent, 100-fs pulse duration, 80-MHz repetition rate) illuminates a motorized variable filter (VF in Fig. 1) and a fast shutter (FS in Fig. 1). Next, the laser beam passes through the scanning system. This system is made of two galvomirrors (VM500, GSI Lumunics) and a telescopic lens pair (L1 and L2 in Fig. 1) that pivot the laser beam from the first galvomirror (GX in Fig. 1) to the second one (GY in Fig. 1). This scanning solution enables a reduction of the mirrors size (6 mm in diameter), and consequently an increase in the scanning velocity, as well as a possibility to integrate a multi spot excitation in the system.[16] See Fig. 1 where L3 and TL pivot the laser beam in back focal plane of the microscope objective (Plan Apo 60X/1.40 Oil, Nikon). Optical sectioning of the sample is achieved using a piezoelectric translator (PZT in Fig. 1). The two-photon emission of the specimen is extracted from the back scattered signal by a dichroic mirror (DM in Fig. 1), and the signal is filtered by an IR blocking filter (BF in Fig. 1), focalized and collected by an avalanche photondiode (APD). All the components of the setup are computer-controlled during microscopy and nanosurgery experiments. Custom-made software was written in LabView (National Instruments). By using subresolution fluorescence beads (60 nm diameter; Bang Labs), we measured the radial and axial resolution of the microscope as 250 and 800 nm, respectively.

3 Results and Discussion

3.1 *Three-Dimensional Microscopy of Microtubules*

Using the experimental setup already described, first, it was possible to make 3-D images of microtubules in living cells. We acquired different optical sections of the cell and the images were analyzed using Matlab (MathWorks) to reconstruct 3-D isosurfaces. Figure 2 shows a 3-D reconstruction of four phases in the yeast cell cycle. The first image [Fig. 2(a)] shows five microtubules in an interphase fission yeast cell. These microtubules are roughly parallel to the longitudinal cell axis of these cylindrically shaped cells. The second image [Fig. 2(b)] shows microtubules in prophase: the long interphase microtubules are absent, whereas a mitotic spindle has formed inside the nucleus. The third image [Fig. 2(c)] shows an anaphase B spindle with two astral microtubules extending from each of the two spindle poles. Figure 2(d) shows the postanaphase array of microtubules and the equatorial microtubule ring. In these images, 1 pixel was equivalent to 50 nm in the *x-y* plane and to 500 nm in the *z* direction. The excitation wavelength was 880 nm, the laser power was 1 mW in the sample, and the integration time for each pixel was 2.5 μs.

3.2 *Nanosurgery on Microtubules*

Moreover, with the same experimental setup it was possible to combine imaging and intracellular nanosurgery on microtubule structures. The experimental procedure was as follows. First, we used the nonlinear microscope to obtained a 3-D reconstruction of the microtubules. Next, using custom-written software, we selected an *xyz* position in the 3-D image that was to be dissected by laser. The software moved the galvomirror and PZT to center the laser beam on the chosen coordinates. The laser power was then increased from 1 to 4 mW (measured in the sample) and the shutter was open for an exposition time of the order of 150 ms. Following the nanosurgery, the laser power was decreased to 1 mW and a time-lapse sequence of 3-D images of microtubules was acquired

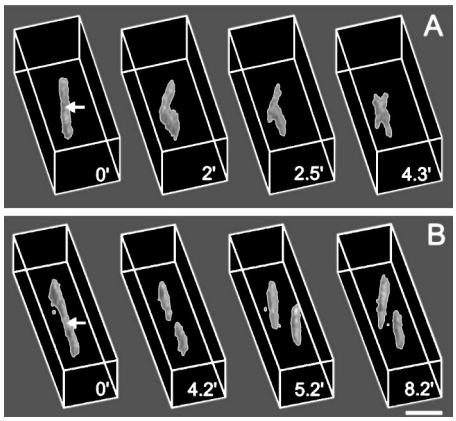

Fig. 3 Nanosurgery on the mitotic spindle in anaphase B with the outcomes when (A) the spindle was irradiated in the middle just after the acquisition of the first image, after which it bent and subsequently broke into two segments that crossed each other forming an X-shaped structure, and (b) the spindle was irradiated in the middle, and subsequently broke into two parts that moved away from each other. The laser power was 4 mW, the exposition time 150 ms, and the wavelength 880 nm; scale bar is 3 μm.

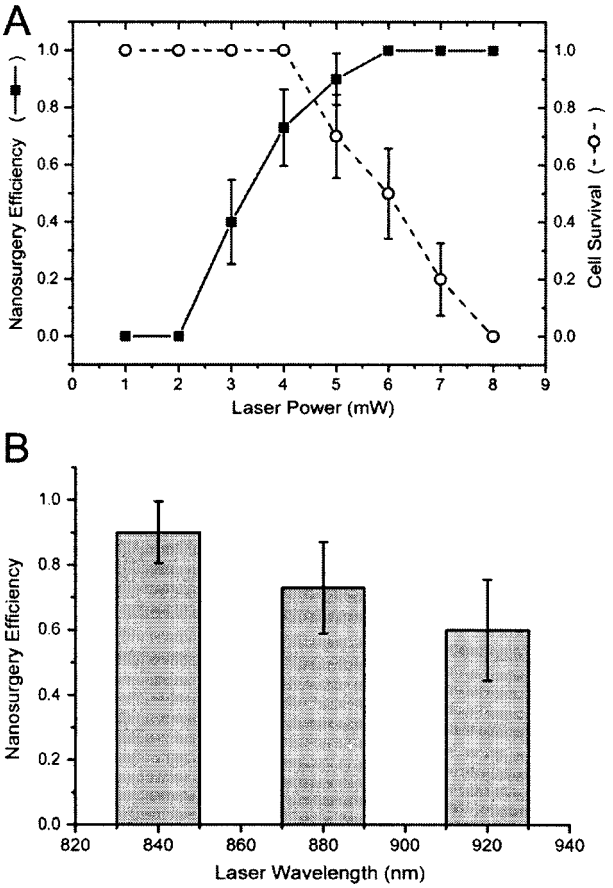

Fig. 4 (a) Dependence of nanosurgery efficiency (full squares) and cell survival (open circles) on the laser power. The exposition time was 150 ms, and the wavelength 880 nm. (b) Dependence of nanosurgery efficiency on laser wavelength. The laser power was 4 mW and the exposition time 150 ms. In both panels the error bars show the theoretical standard deviation for a binomial distribution. The number of measurements was 10 for each laser power in (a) and each wavelength value in (b).

to visualize the dynamics of the effect of nanosurgery. Figure 3 shows two examples of a nanosurgery on the mitotic spindle in anaphase B. The spindle shown in Fig. 3(a) was irradiated in the middle at a time between the acquisition of the first two images, after which it bent and subsequently broke into two segments that crossed each other forming an X-shaped structure. The spindle in Fig. 3(b) was also irradiated in the middle, and subsequently broke into two parts that moved away from each other. These images indicate that the cutting of the spindle was complete. Furthermore, small random movements of the two segments, which were observed for 20 min following the nanosurgery, suggest that the segments were disconnected. It would be useful to visualize the damaged spindle and check the spatial distribution of tubulin structures by tubulin immunodetection on cells fixed immediately after the nanosurgery.

In the nanosurgery experiment, it is crucial to use an optimal combination of the laser power and exposition time. We explored how the efficiency of nanosurgery depends on the laser power. We varied the laser power, while the laser wavelength was fixed at 880 nm and the exposition time at 150 ms [Fig. 4(a)]. This experiment was performed on cytoplasmic microtubules in interphase cells. In the case of low laser powers (<2 mW), we did not observe a change in the microtubule shape, length, or location. We assume that, in this case, laser-induced photobleaching of the fluorescence probes only at the site of irradiation. At laser powers above 2 mW, we observed clear breakage of the microtubules. The irradiated microtubule broke into two segments, which were not aligned with the initial microtubule axis. One of the segments often depolymerized. The frequency of breakage events increased with increasing laser power, and saturated above 6 mW. At high laser powers (4 to 8 mW), besides local microtubule breakage, we sometimes observed an explosion of the microtubule structure and immediate cell damage. The frequency of explosion events f_{expl} increased with the laser power and saturated above 8 mW. Cell survival, estimated as $1-f_{\mathrm{expl}}$, is also shown in Fig. 4(a). Considered together, the nanosurgery efficiency and the cell survival curves indicate that the optimal laser power for nanosurgery experiments is about 4 mW. At this power, the cell survival is 100%, whereas the nanosurgery efficiency is 75%. A very similar dependence of the nanosurgery efficiency on the laser power was found when nanosurgery was performed on the spindle instead of cytoplasmic microtubules. In an analogous but less detailed test, we found that the optimal exposition time is 150 ms by varying the exposition time and keeping the laser power constant at 4 mW.

Next, we fixed the laser power at 4 mW and the exposition time at 150 ms, and varied the wavelength. The efficiency of the nanosurgery decreased from $\lambda=840$ to 920 nm [Fig. 4(b)]. Since the nanosurgery efficiency decreases (see later in the paper), whereas the GFP two-photon cross section increases with increasing wavelength in this interval,[2] we chose the intermediate value of 880 nm for the combined imaging and nanosurgery experiments.

3.3 *Viability of Cells After Nanosurgery*

An important issue in nanosurgery experiments is the extent of damage to the cell. The cells irradiated at a low laser power (up to 4 mW) did not show any visible damage besides the breakage of the irradiated microtubule structure. The cells were found to be alive and healthy during the whole observation time (typically 1 h after the nanosurgery), as judged by the characteristic motion of intracellular granules similar to that of intact cells. When the nanosurgery was performed on dividing cell, the process of cell division continued and finished successfully. The spindles that were broken by the nanosurgery recovered, a postanaphase array of microtubules formed, followed by a septum and two normal daughter cells.[12]

3.4 *Interpretation of the Physical Aspects of Nanosurgery*

In the following, we describe a set of results that can help to determine the physical mechanism underlying nanosurgery. First, we tried to perform nanosurgery with the titanium-sapphire laser in continuous-wave (cw) mode at the same laser power as used before with a mode-locked (ML) laser, 4 mW in the sample. We were not able to induce microtubule brakeage in this case, which suggests that the laser nanosurgery is essentially due to nonlinear absorption processes.

To discern whether the laser nanosurgery is due to the absorption of GFP or of another kind of molecule, we performed two tests. In the first test, we applied nanosurgery on the region of the cell without visible GFP, using a high laser power (7 mW). Although the laser at this power induced an explosion in 80% of cases when targeted at a GFP-containing structure [Fig. 4(a)], explosion was not observed when a region devoid of GFP was targeted (0 out of 10 trials). In the second experiment, nanosurgery was performed on the same type of cell as before, but with the nuclear membrane marked with GFP, instead of using GFP-tagged tubulin. Since the nuclear membrane encloses the spindle tightly, it is possible to know the position of the spindle in the cells with a labeled nuclear membrane, without labeling the spindle directly. Nanosurgery performed on the spindle in these cells did not induce any variation in the shape of the nuclear membrane enclosing the spindle, which implies that the spindle shape did not change either (Fig. 5). The results of both experiments suggest that the laser nanosurgery is due to the two-photon absorption of GFP. Therefore, the microtubule breakage is due to thermal relaxation of the excess vibrational energy deposited in the vibronic manifold by the two-photon absorption.

The observed dependence of the nanosurgery efficiency on the laser power and wavelength can be explained by two-photon absorption of GFP. Two-photon absorption increases quadratically with laser power. However, the regime of exposition time and laser power necessary for an efficient nanosurgery is in the saturation part of the absorption curve. Hence, the observed dependence of the efficiency on the laser power does not display a quadratic dependence, but only the saturation part. Furthermore, when the laser wavelength is decreased while keeping the power constant, the amount of excess vibrational energy deposited in the sample increases. As a consequence, greater local heating is produced by the thermal relaxation of the vibrational levels, with an increasing nanosurgery efficiency.

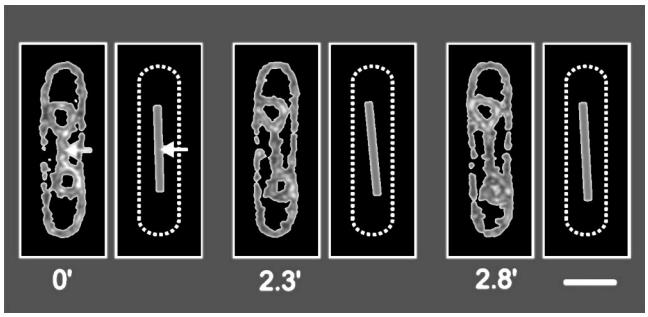

Fig. 5 Nanosurgery on a yeast cell in which the nuclear membrane (not tubulin) is labeled with GFP. Three images are shown, each represents a single optical section. Time in minutes is noted. To the right of each of the images is a scheme showing the position of the spindle (solid line) and the cell membrane (dotted line). Nanosurgery was performed on the center of the spindle after the acquisition of the first image. The nanosurgery did not induce any variation in the shape of the nuclear membrane enclosing the spindle, which suggests that the spindle shape did not change either. Scale bar is 4 μm.

If the nanosurgery is due to the two-photon absorption of GFP, the nanosurgery volume is of the order of the two-photon excitation (TPE) volume. Theoretically, we can estimate this volume as $V_{\mathrm{TPE}}=\pi^{3/2}\omega_{XY}^2\omega_Z$, where ω_{XY} and ω_Z are the $1/e$ width of the lateral (xy) and axial (z) intensity square profiles.[2] For our setup with $\omega_{XY}=150\,\mathrm{nm}$ and $\omega_Z=350\,\mathrm{nm}$, the volume is 0.1 fl. Moreover, using a laser power of 4 mW, we usually observed a dark spot of the same order of the two-photon microscopy resolution at the location of the nanosurgery immediately after the nanosurgery, which is consistent with a subresolution nanosurgery volume.

Taken together, our data are consistent with the hypothesis that nanosurgery is due to two-photon absorption of GFP. Additional work may be necessary to further clarify physical aspects of nanosurgery. This is, however, beyond the scope of this study, the goal of which was to characterize the method for microscopy and nanosurgery on microtubule structures in living cells.

4 Conclusion

NIR femtosecond laser pulses can be used for both microscopy and nanosurgery on fluorescently labeled structures within living cells. Nanosurgery can be performed with submicrometer precision and without visible collateral damage to the cell. The nanosurgery on the structures labeled with GFP is most likely due to two-photon absorption of GFP molecules.

Acknowledgments

We thank Y. Hiraoka for the GFP fusion constructs, G. Thon for cell transformation and discussion of yeast biology, and R. Righini for discussion of nonlinear absorption. This work was supported by LENS Contract No. HPRI-CT-1999-00111 CE and by the Ente Cassa di Risparmio di Firenze.

References

1. W. Denk, J. H. Strickler, and W. W. Webb, ''Two-photon laser scanning fluorescence microscopy,'' *Science* **248**, 73–76 (1990).
2. W. R. Zipfel, R. M. Williams, and W. W. Webb, ''Nonlinear magic: multiphoton microscopy in the biosciences,'' *Nat. Biotechnol.* **21**, 1369–1377 (2003).
3. W. R. Zipfel, R. M. Williams, R. Christie, A. Y. Nikitin, B. T. Hyman, and W. W. Webb, ''Live tissue intrinsic emission microscopy using multiphoton-excited native fluorescence and second harmonic generation,'' *Proc. Natl. Acad. Sci. U.S.A.* **100**, 7075–7080 (2003).
4. M. J. Miller, S. H. Wei, I. Parker, and M. D. Cahalan, ''Two-photon imaging of lymphocyte motility and antigen response in intact lymph node,'' *Science* **296**, 1869–1873 (2002).
5. S. Maiti, J. B. Shear, R. M. Williams, W. R. Zipfel, and W. W. Webb, ''Measuring serotonin distribution in live cells with three-photon excitation,'' *Science* **275**, 530–532 (1997).
6. G. Isenberg, W. Bielser, W. Meier-Ruge, and E. Remy, ''Cell surgery by laser micro-dissection: a preparative method,'' *J. Microsc.* **107**, 19–24 (1976).
7. J. R. Aist and M. W. Berns, ''Mechanics of chromosome separation during mitosis in *Fusarium (Fungi imperfecti)*: new evidence from ultrastructural and laser microbeam experiments,'' *J. Cell Biol.* **91**, 446–458 (1981).
8. R. J. Leslie and J. D. Pickett-Heaps, ''Ultraviolet microbeam irradiations of mitotic diatoms: investigation of spindle elongation,'' *J. Cell Biol.* **96**, 548–561 (1983).
9. A. Khodjakov, R. W. Cole, and C. L. Rieder, ''A synergy of technologies: combining laser microsurgery with green fluorescent protein tagging,'' *Cell Motil. Cytoskeleton* **38**, 311–317 (1997).
10. K. Konig, I. Riemann, and W. Fritzsche, ''Nanodissection of human chromosomes with near-infrared femtosecond laser pulses,'' *Opt. Lett.* **26**, 819–821 (2001).
11. U. K. Tirlapur and K. Konig, ''Femtosecond near-infrared laser pulses as a versatile non-invasive tool for intra-tissue nanoprocessing in plants without compromising viability,'' *Plant J.* **31**, 365–374 (2002).
12. I. M. Tolic-Nørrelykke, L. Sacconi, G. Thon, and F. S. Pavone, ''Positioning end elongation of the fission yeast spindle by microtubule-based pushing,'' *Curr. Biol.* **14**, 1181-1186 (2004).
13. I. M. Hagan, ''The fission yeast microtubule cytoskeleton,'' *J. Cell. Sci.* **111**, 1603–1612 (1998).
14. D. Q. Ding, Y. Chikashige, T. Haraguchi, and Y. Hiraoka, ''Oscillatory nuclear movement in fission yeast meiotic prophase is driven by astral microtubules, as revealed by continuous observation of chromosomes and microtubules in living cells,'' *J. Cell. Sci.* **111**, 701–712 (1998).
15. D. Q. Ding, Y. Tomita, A. Yamamoto, Y. Chikashige, T. Haraguchi, and Y. Hiraoka, ''Large-scale screening of intracellular protein localization in living fission yeast cells by the use of a GFP-fusion genomic DNA library,'' *Genes Cells* **5**, 169–190 (2000).
16. L. Sacconi, E. Froner, R. Antolini, M. R. Taghizadeh, A. Choudhury, and F. S. Pavone, ''Multiphoton multifocal microscopy exploiting a diffractive optical element,'' *Opt. Lett.* **28**, 1918–1920 (2003).